# Pore Size Evaluation for Fine Porous Freeze-Dried Cellulose Acetate Membrane by Gas Separation

A. TANIOKA and K. ISHIKAWA,* *Tokyo Institute of Technology, 2-12-1, Ookayama Meguro-ku, 152 Tokyo, Japan,* and A. KAKUTA, M. KURAMOTO, and M. OHNO, *Nuclear Engineering Laboratory, Toshiba Corp., 4-1, Ukishimacho, 210 Kawasaki, Japan*

## Synopsis

The pore size for a fine porous freeze-dried cellulose acetate membrane was evaluated by gas separation methods, where the Present–deBethune equation was applied. Separation coefficients were referred to the calculated value for each pore size from this equation. Nuclepore, Millipore VS, and Millipore VC, whose pore sizes were already known by bubble point method, were tested for this method. Pore diameters for this cellulose acetate membrane, thus determined, were about 25 and 40 Å from Ar–Kr and $N_2$–Kr separation systems, respectively, which agreed well with the results from electron microscope (50 Å) and $N_2$ gas permeability (50 Å). However, it is impossible to apply this method to He gas separation, since He gas permeability is higher than the expected value as Knudsen flow, which indicates that some channels are existing in this membrane, where He gas is more permeable than the other gases.

## INTRODUCTION

A freeze-dried cellulose acetate membrane with high permeability and high separation factor was prepared.[1] Gas permeabilities for such a membrane were inversely proportional to the square root of molecular weights of gases, suggesting that the gas flow mechnism through this membrane was Knudsen flow. This membrane was porous.[2,3] The mean pore size, calculated from $N_2$ gas permeabilities using Yasuda and Tsai's equation,[4] was about 50 Å in diameter. The structure was observed with an ultrathin sectioning electron microscope. It was found that the membrane had an asymmetric structure, which was composed of top thin layer (skin layer) and bottom thick layer (matrix layer).[5] The fine structure on the top surface was a network that consisted of about 50 Å pores. The bottom layer also gave a network structure among pores, whose diameters were more than 0.3 μm. Gas transport characteristics are mainly determined by the skin layer.

This membrane is applicable for inert gas separation as shown in the previous paper,[6,7] since the gas flow mechanism is Knudsen flow, where the separation factor is equal to the square root of the molecular weight ratio of two different gases, which is called the ideal separation factor. However, separation factors for all gases in this experiment were smaller than ideal ones. Such a deterioration concerning the porous media was already predicted from the theoretical considerations reported by Present and de-

*Present address; Ochanomizu Women's University, Ootsuka Toshima-ku, 152 Tokyo, Japan.

Bethune,[8] who assume the possibility of collision between different molecules in the pore, even if it is Knudsen flow. A separation factor is a function of pore size and gas pressure in their treatment and is calculated at various pressures and pore sizes by using a computer. Experimental results were referred to calculated results to decide the pore size. This is one of the methods to evaluate the pore size for a porous polymer membrane.

The authors encountered great difficulty in measuring the pore size for porous polymer, provided that it is less than 100 Å. However, it is possible to measure such a small pore size, using the gas separation method cited above. In a previous paper, the authors estimated it as about 50 Å for a fine porous cellulose acetate membrane from gas permeability measurements and electron microscope observation. In this study, the authors intended to determine the pore size using a gas separation experiment.

## EXPERIMENTAL

### Materials

Fine porous cellulose acetate membrane was prepared from a mixed solution of formamide, acetone and cellulose acetate (Eastman Chemical Co. Ltd., E398-3) by the casting method, as cited in a previous paper. The membrane pore diameter was about 50 Å, measured from $N_2$ gas permeabilities and electron microscope observation.

Gas permeability coefficients and separation factors for commercial Nuclepore, Millipore VS, and Millipore VC filters were measured to discuss the validity of theoretical considerations. Average pore diameters, measured by bubble point method, were 200, 600, and 1000 Å, respectively.

### Gas Permeability and Separation Measurements

Figure 1 shows an apparatus layout for permeability and separation factor measurements, which were a little improved in comparison with the measurements reported by Agrawal and Sourirajan.[9] Permeability measurements were made in accordance with the following experimental procedures. Gases are fed into the high pressure side and transported to the low
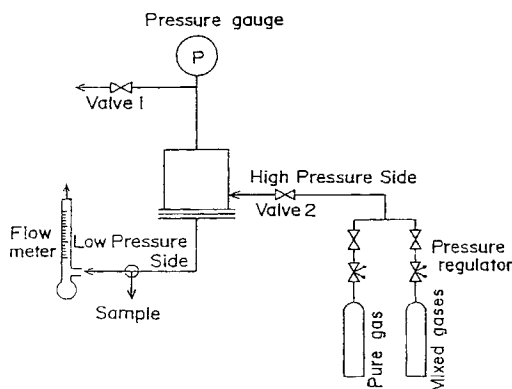


Fig. 1.  Gas permeability testing apparatus.

pressure side through the membrane. The gas flow rate at the low pressure side is measured by a gas flow meter. Gas flux can generally be expressed by

$$J = -K(p_B - p_F)/L \tag{1}$$

where $K$ is the permeability coefficient, $p_F$ is pressure on the high pressure side, and $p_B$ is pressure on the low pressure side. In this experiment, $p_B$ was always 1 atm.

Separation factor measurement was carried out by the following experimental procedures. The mixed gases, in which the molar fraction of a based gas is 99.5% and that of the gas to be separated is 0.05%, are supplied into the high pressure side. The mixed gas on this side is leaked from valve 1 to maintain a constant molar fraction. The pressure on the high pressure side is always constant. The permeated mixed gas compositions were measured by gas chromatography after sampling with a syringe. The pressure on the low pressure side always stays at 1 atm. Temperature during measurements was 25°C. The separation factor is defined as

$$\alpha = (x_B/1 - x_B)/(x_F/1 - x_F) \tag{2}$$

where $x_B$ and $x_F$ are molar fractions of marked light gas in the low pressure side and the high pressure side, respectively.

## RESULTS AND DISCUSSION

In Figure 2, gas permeability coefficients for $H_2$, He, $N_2$, and Ar are plotted as functions of mean pressures on high and low pressure sides [$\bar{p} = (p_B + p_F)/2$]. Permeability coefficients increase with increase in mean pressures and are expressed by[10,11]

$$K = K_0 + (B_0/\eta)\bar{p} \tag{3}$$

where $K_0$ is the Knudsen permeability coefficient, which is inversely proportional to the square root of molecular weight $M$ for the gas, $\eta$ is gas viscosity, and $B_0$ is a geometrical factor of the membrane. The coefficient $K_0$ can be estimated by an extrapolation of $K$ vs. $\bar{p}$ to $\bar{p} = 0$, and $B_0/\eta$ is obtained from the slope. In Figure 3, gas permeabilities for $H_2$, He, $N_2$, Ar, and Kr for Nuclepore are plotted as a function of mean pressure. In Figures 4 and 5, permeabilities for He, $N_2$, $O_2$, Ar, and Kr gases are also plotted for Millipore VS and VC filters, respectively. These are also expressed by eq. (1). Their slopes increase with pore size increase. If the pore size increases, the separation efficiency will decrease as a consequence of dominating viscous flow.

In Table I, the separation factors for fine porous cellulose acetate membrane are shown for mixed gases, $H_2$-He, Ar-Kr, $N_2$-Kr, He-$N_2$, $H_2$-Ne, He-Ar, and He-Kr. Mixed gases combinations are listed in the first column. The former gas concentration was 99.5% in the high pressure side, which was called the base gas. In other words, the separation factor presents the
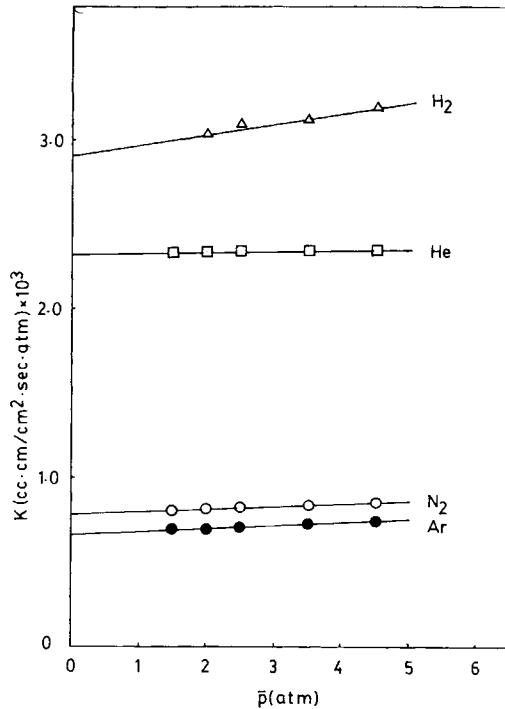
Fig. 2.   Gas permeability coefficients for $H_2$, He, $N_2$, and Ar as a function of mean pressure for cellulose acetate membrane.

extent of the lighter gas condensation. Ideal separation factors are shown in the second column, which are the square root of the two different gases molecular weight ratio. The measured separation factor is lower than ideal value, because of the viscous flow effect. In Figure 6, separation factors for $N_2$–Kr are plotted as a function of the pressure on the high pressure side (feed pressure). If gas pressure were 1 atm with the same mixed gas composition on both sides of the membrane, the separation factor was unitary, since there was no flow and separation. It increased with feed pressure $p_F$ below 4 atm before decreasing above 5 atm. $N_2$–Kr separation coefficients for Nuclepore, Millipore VS, and Millipore VC are also plotted in Figure 6. These indicated that the separation coefficient decreased, when the feed pressure and pore size increased. If the flow through membrane is Knudsen flow, component molar velocity is proportional to the difference in partial pressure between inflow and outflow[12]:

$$G_1 = A_{G_1}(p_F x_F - p_B x_B) = A_{G_1} p_F (x_F - \gamma x_B) \qquad (4)$$

$$\begin{aligned} G_2 &= A_{G_2}[p_F(1 - x_F) - p_B(1 - x_B)] \\ &= A_{G_2} p_F[(1 - x_F) - \gamma(1 - x_B)] \end{aligned} \qquad (5)$$

where $\gamma = p_B/p_F$ and $p_F$ and $p_B$ are pressures on the high and low pressure sides, respectively. $x_F$ and $x_B$ are the molar fraction of component 1 in high and low pressure sides, respectively. $A_{G_1}$ and $A_{G_2}$ are permeabilities for pure gases for components 1 and 2, respectively, and are written as follows:
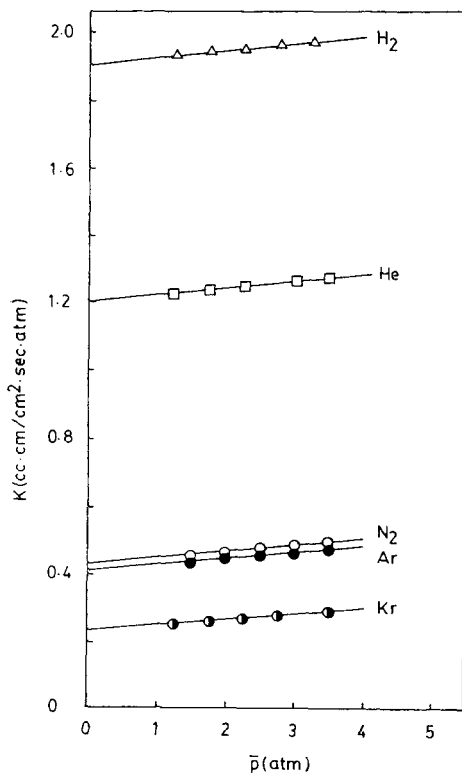
Fig. 3.  Gas permeability coefficients for $H_2$, He, $N_2$, Ar, and Kr as a function of mean pressure for Nuclepore.

$$A_{G_1} = a/(M_1)^{1/2}, \quad A_{G_2} = a/(M_2)^{1/2} \qquad (6)$$

where $a$ is constant. In this experiment, the light gas molar fraction on the low pressure side is defined as

$$x_B = G_1/(G_1 + G_2) \qquad (7)$$

From Eqs. (4), (5), and (7), the following relation is formed between $x_F$ and $x_B$:

$$x_B/1 - x_B = G_1/G_2 = a_0(x_F - \gamma x_B)/[(1 - x_F) - \gamma(1 - x_B)] \qquad (8)$$

When pressure on the low pressure side is very small $(p_B/p_F \to 0)$,

$$\frac{x_B}{1 - x_B}\bigg/\frac{x_F}{1 - x_F} = (M_2/M_1)^{1/2} = A_{G_1}/A_{G_2} = a_0 \qquad (9)$$

If ideal separation factor $a_0$ is defined, molar fraction on the high pressure side is confirmed as $x_F^0$ and from eq. (9)

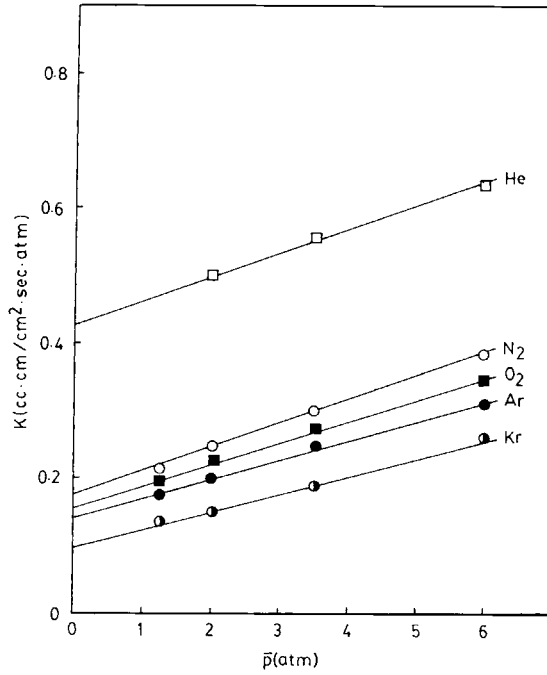$$x_F^0 = x_B/[x_B + a_0(1 - x_B)] \qquad (10)$$

Fig. 4.  Gas permeability coefficients for He, $N_2$, $O_2$, Ar, and Kr as a function of mean pressure for Millipore VS.
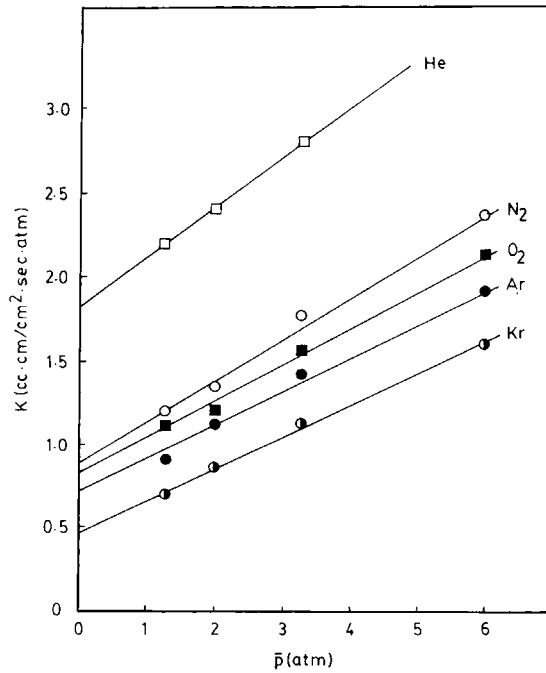


Fig. 5.  Gas permeability coefficients for He, $N_2$, $O_2$, Ar, and Kr as a function of mean pressure for Millipore VC.

TABLE I
Separation Factors for Freeze-dried Cellulose Acetate Membrane

| Mixed gases | $\alpha_0 = \sqrt{M_2/M_1}$ | $p_F$ (pressure on high pressure side) (atm) | | | | |
|---|---|---|---|---|---|---|
| | | 2.0 | 3.0 | 4.0 | 6.0 | 8.0 |
| $H_2$–He | 1.41 | 1.14 | 1.15 | 1.17 | 1.19 | 1.20 |
| Ar–Kr | 1.45 | 1.20 | 1.25 | 1.29 | 1.23 | 1.29 |
| $N_2$–Kr | 1.73 | 1.32 | 1.39 | 1.43 | 1.42 | 1.39 |
| He–Ne | 2.25 | 1.63 | 1.98 | 1.92 | 1.96 | 2.00 |
| $H_2$–Ne | 3.16 | 1.88 | 2.20 | 2.27 | 2.32 | 2.33 |
| He–Ar | 3.16 | 2.07 | 2.26 | 2.35 | 2.14 | 2.58 |
| He–Kr | 4.58 | 2.81 | 3.44 | 3.68 | 3.66 | 3.55 |

Here, separation efficiency $Z$ is defined as

$$Z = (x_B - x_F)/(x_B - x_F^0) \qquad (11)$$

$x_F$ and $x_F^0$ from eqs. (8) and (10) are substitute into eq. (11),

$$Z = 1 - \gamma \qquad (12)$$

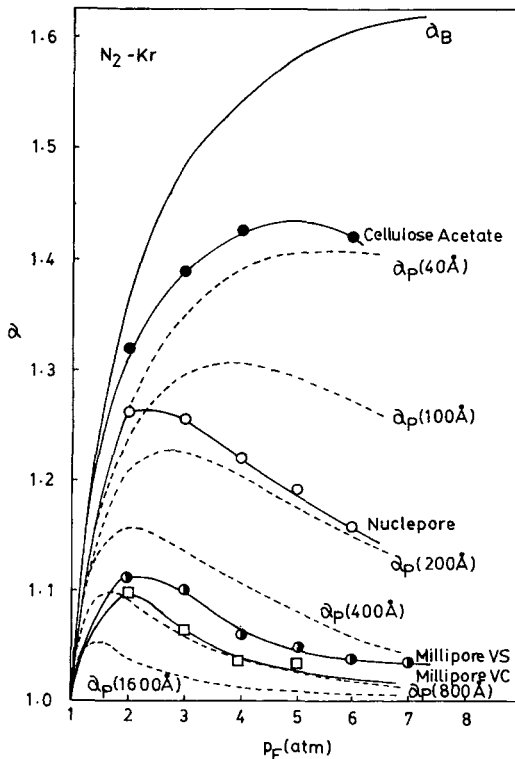Equation (12) indicates that separation efficiency will be decreased only



Fig. 6. Separation coefficients for cellulose acetate, Nuclepore, Millipore VS, and Millipore VC, and $\alpha_B$ and the test of the Present–deBethune equation (—) on $N_2$–Kr system for each pore size.

back flow from the low pressure side, if the flow is ideally Knudsen flow. When $x_F$ and $x_F^0$ from eqs. (2) and (10) are substituted into eq. (12),

$$Z = (\alpha - 1)[x_B + \alpha_0(1 - x_B)]/(\alpha_0 - 1)[x_B + \alpha(1 - x_B)] \qquad (13)$$

In these experiments, $x_F = 0.995$, $1 - x_F = 0.005$, and $(\alpha_0/\alpha) < 5$

$$[x_B + \alpha_0(1 - x_B)]/[x_B + \alpha(1 - x_B)] \simeq 1$$

Then eq. (13) becomes

$$Z = (\alpha - 1)/(\alpha_0 - 1) \qquad (14)$$

Separation factor $\alpha_B$, when considering what only the back flow effect becomes from eqs. (12) and (14),

$$\alpha_B = 1 + (\alpha_0 - 1)(1 - \gamma) \qquad (15)$$

Equation (15) shows that separation factors were not ideal, in spite of Knudsen flow, since the back flow effects from the low pressure side, which was indicated in eqs. (4) and (5), should be considered, since the pressure on the low pressure side was always 1 atm. These effects were predominant at the low feed pressure. In Figure 6, $\alpha_B$ values are plotted as a function of feed pressure. $\alpha_B$ values were higher than experimental results values over the whole pressure range.

If the pore size or the feed pressure increased, which corresponded to a decrease in the mean free path, the flow through the porous membrane not only became the ideal Knudsen flow, but also contained viscous flow, as shown in Figures 2–5. Even if the flow is the ideal Knudsen flow, collisions among different gases in mixed gases should be considered in the membrane pores. These collisions are called Present–deBethune effects. The viscous and Present–deBethune flow reduced the separation efficiency. Taking these flows into account, Present and deBethune decided separation efficiency $Z_p$ as follows[8]:

$$Z_p = \frac{\int_{\phi_B}^{\phi_F} \exp\{[(1 + \alpha_0 f/b)\,\phi + (f/2)\,\phi^2]/b\}\,\mathrm{d}\phi}{\phi_F \exp\{[(1 + \alpha_0 f/b)\,\phi_F + (f/2)\,\phi_F^2]/b\}} \qquad (16)$$

where

$$\phi = \frac{3\bar{r}p}{64\eta}\sqrt{\frac{\pi M_2}{2RT}} \qquad (17)$$

$$b = x_B + \alpha_0(1 - x_B) \qquad (18)$$

$$f = \frac{256}{9\pi}\frac{b}{\alpha_0^2}\,[x_B + (1 - x_B)\alpha_0^2]\,\frac{\eta}{\rho D_{12}} \qquad (19)$$

where $\bar{r}$ is the pore radius, $p$ is pressure, $\eta$ is gas viscosity, $\rho$ is gas density,

and $D_{12}$ is the mutual diffusion coefficient for gas. $Z_p$ was calculated by computer programs.

The separation factor $\alpha_p$, which is calculated from the Present–deBethune eqs. (16) and (14), is

$$\alpha_p = 1 + (\alpha_0 - 1)Z_p \qquad (20)$$

In Figure 6, $\alpha_p$ values are plotted as a function of pressure. Every curve has a maximum. If all the flows were expressed by Knudsen equation, separation coefficients were $\alpha_B$ values, as shown in eq. (15). On the other hand, viscous flow would become predominant with increasing feed pressure to reduce the separation coefficient. Products of two effects make a maximum. At the same time, the diameters of membrane pores are also shown with $\alpha_p$ in Figure 6. The experimental curves are able to be referred to the calculated one by eq. (20). Pore diameters thus determined were 200, 600, and 800 Å for Nuclepore, Millipore VS, and Millipore VC filters, respectively. They agree well with the results determined by bubble point method, which were 200, 600, and 1000Å, respectively. It is assumed that the Present–deBethune equation is applicable to this study. The cellulose acetate pore diameter was referred to 40 Å, which agreed well with the size determined by electron microscopic observation (50 Å) and $N_2$ gas permeability measurements (50 Å). This pore size determination method was adaptable to other gas separation data. In Figure 7, separation factors for
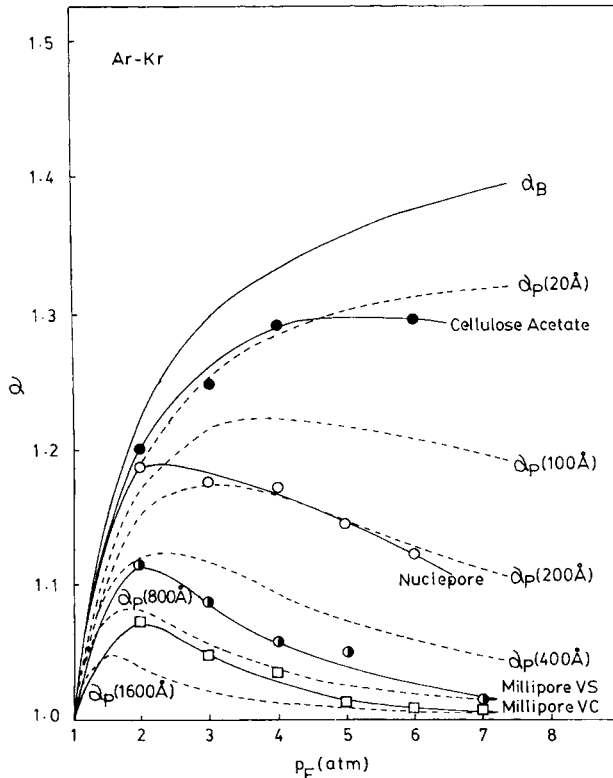


Fig. 7. Separation factors for various membranes and $\alpha_B$ and the test of the Present–deBethune equation on Ar–Kr system.

Ar–Kr are also shown for those membranes. Values calculated by the Present–deBethune equation are also shown as dotted lines. Pore sizes for Nuclepore, Millipore VS, and Millipore VC filters from this figure were 200, 600, and 1000 Å, respectively, and agreed well with results cited above. However, cellulose acetate pore diameter was 25 Å and smaller than the above determined values. It is considered that such a value is in error, since eq. (16) is very sensitive to each parameter in the small pore size region.

## He Gas Separation

In Figure 8, separation factors for He–Kr gases are shown for each porous membrane. The values calculated by the Present–deBethune equation are also plotted in Figure 9 with dotted line. Pore diameters for Nuclepore, Millipore VS, and Millipore VC were 80, 200, and 400 Å, respectively. All of them were less evaluated, since parameters applied in eq. (16 ) were not appropriate to the calculation of He–Kr separation factors. If arbitrary parameters are chosen in the calculation, reasonable pore size could be obtained. However, those parameters cannot be changed, since they were already determined experimentally. In Figure 8, separation factors for cellulose acetate membrane were also shown as a function of feed pressure. They agreed well with $\alpha_B$ values below 4 atm and became lower than $\alpha_B$ values above 4 atm, which indicated that the Present–deBethune effects could be seen. In Figures 9 and 10, separation factors for He–Ne and He–
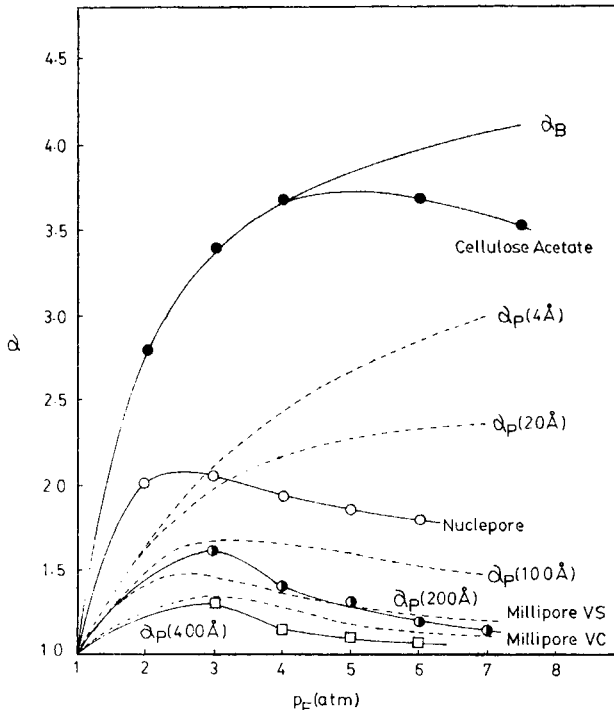


Fig. 8. Separation factors for various membranes and $\alpha_B$ and the test of the Present–deBethune equation on He–Kr system.
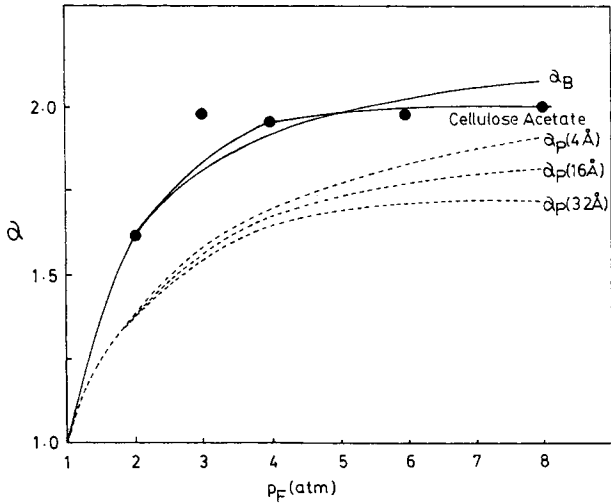
Fig. 9.   Separation factors for cellulose acetate membrane, $\alpha_B$, and the test of the Present–deBethune equation on He–Ne system.

Ar gases for cellulose acetate membrane are plotted as a function of feed pressure, with separation factors calculated by the Present–deBethune equation. Experimental values coincided with $\alpha_B$ at low feed pressures and otherwise took lower values than $\alpha_B$, which were similar to He–Kr separation data. The presumed pore diameter from these results was less than 4 Å. This pore size was very small, compared with what was determined by other methods. Even if the parameters in eq. (16) were revised to better ones, larger pore sizes, as great as 50 Å, cannot be obtained, since experimental values are very close to the upper limit of separation factor $\alpha_B$. Such a high separability indicates that the possibility of collisions between He and the other gas is lower than expected, which presumes the existence
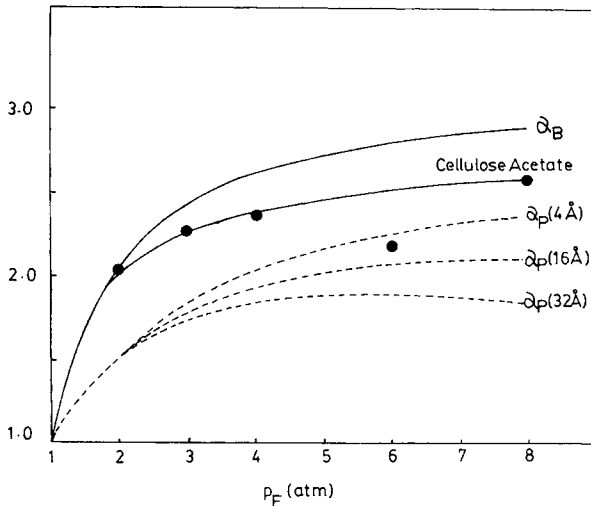


Fig. 10.   Separation factors for cellulose acetate membrane, $\alpha_B$, and the test of the Present–deBethune equation on He–Ar system.
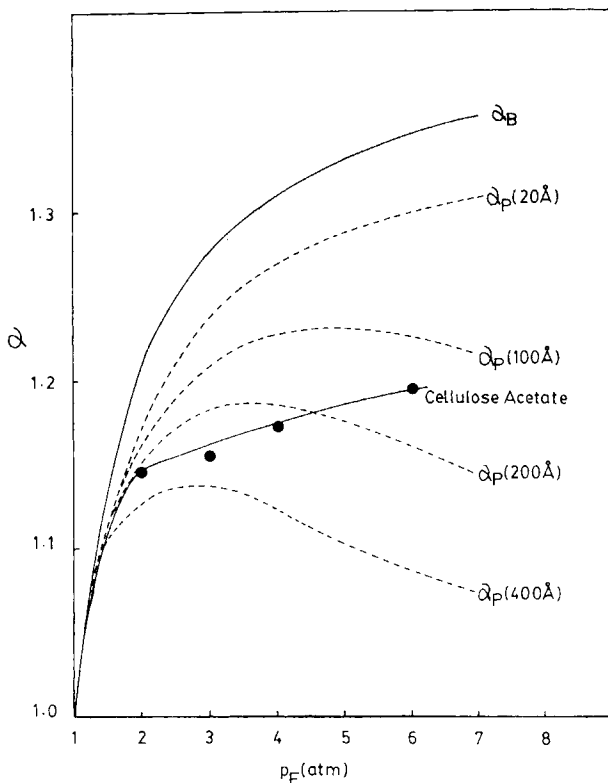
Fig. 11. Separation factors for cellulose acetate membrane, $\alpha_B$, and the test of the Present–deBethune equation on $H_2$–He system.

of a small space where only He molecules are permeable. $K_0$ values for different gases in Figure 2 are almost inversely proportional to the square root of molecular weight, but the $K_0$ value for He is higher than the expected value, which supports the above idea. In Figure 11, separation factors for $H_2$–He are plotted for cellulose acetate with curves calculated by eq. (20). Pore diameter from this figure was about 200 Å, which was four times larger than that from other experiments. $H_2$ gas was not condensed as expected from eq. (16), since the He gas permeability for this membrane was greater than that which was expected from Knudsen flow. It was suggested that the channels, where He gas was more permeable than $H_2$, were existing in this membrane. This idea was supported from the results wherein the He gas permeability for homogeneous dense cellulose acetate membrane was larger than that for $H_2$, even if $H_2$ molecular weight was smaller than that for He and even if $H_2$ solubility parameter was larger than that for He.[13–15] It is concluded that He gas cannot be used in the pore size determination from gas separations.

## References

1. A. Tanioka, K. Ishikawa, A. Kakuta, M. Kuramoto, and M. Ohno, *J. Appl. Polym. Sci.*, **29**, 583 (1984).
2. S. A. Stern and A. H. DeMeringo, *J. Polym. Sci., Polym. Phys. Ed.*, **16**, 735 (1978).

3. W. Pusch and A. Tanioka, *Desalination,* **46**, 425 (1983).

4. H. Yasuda and J. T. Tsai, *J. Appl. Polym. Sci.,* **18**, 805 (1974).

5. A. Kakuta, M. Kuramoto, M. Ohno, H. Kushida, A. Tanioka, and K. Ishikawa, *J. Polym. Sci., Polym. Chem. Ed.,* **18**, 3229 (1980).

6. S. Kimura, et al., *Radiochem. Radional. Lett.,* **13**, 354 (1973).

7. A. Tanioka, A. Kakuta, O. Ozaki, M. Ohno, and K. Ishikawa, *Kobunshi Ronbunshu, Jpn.,* **34**, 807 (1977).

8. R. D. Present and A. J. deBethune, *Phys. Rev.,* **75**, 1050 (1949).

9. J. P. Agrawal and S. Sourirajan, *J. Appl. Polym. Sci.,* **14**, 1303 (1970).

10. H. Adzumi, *Bull. Chem. Soc. Jpn.,* **12**, 285 (1938).

11. P. G. Carman, *Flow of Gases through Porous Media,* Butterworths, London, 1956.

12. M. Benedict and T. H. Pigford, *Nuclear Chemical Engineering,* McGraw-Hill, New York, p. 489.

13. S. T. Hwang and K. Kammermeyer, *Can. J. Chem. Eng.,* 82 (1966).

14. Y. Ito, *Kobunshi Kagaku,* **18**, 124 (1961).

15. J. Crank and G. S. Park, *Diffusion in Polymers,* Academic, New York, 1968.